

# Characterization of Mixing in Micromixers by a Test Reaction: Single Mixing Units and Mixer Arrays

Wolfgang Ehrfeld, Klaus Golbig, Volker Hessel,\* Holger Löwe, and Thomas Richter

*Institut für Mikrotechnik Mainz GmbH, Carl-Zeiss-Strasse 18-20, D-55129 Mainz-Hechtsheim, Germany*

The mixing quality of a single mixing unit and mixer arrays having various designs was characterized. A known test reaction for mixing quality had to be optimized, since a much higher sensitivity as for the characterization of macroscopic mixers was needed. This adapted test reaction allowed not only the characterization of the mixing quality but also analysis of the homogeneity of the flow distribution between parallelly aligned mixing units. A comparison of the mixing quality to those of macroscopic reference systems (like mixing in stirred and unstirred vessels as well as to laminar and turbulent mixing-tees) is presented. The mixing quality–volume flow dependence revealed a complex behavior, the hydrodynamic origin of which has been analyzed.

## Introduction

Although some microfluidic components for analytical purposes (Mathies, 1995; Widmer, 1994) have been investigated for many years, micromachining technologies have only recently been applied for the design of miniaturized devices for synthetic applications, so-called microreactors (Ehrfeld, 1996; Benson, 1993; Gravesen, 1996; Hönicke, 1996; Kämper, 1997; Lerou, 1996; Richter, 1997; Schubert, 1993; Shaw, 1996; Wegeng, 1996). The main components of such microreactors are mixers and heat exchangers. A considerable choice of different types of static mixers has been reported (Branebjerg, 1996; Gravesen, 1996; Hessel, 1998; Mensinger, 1995; Möbius, 1995; Schwesinger, 1996; Wegeng, 1996). Almost all of them use the principle of multilamination to achieve fast mixing via diffusion. This is the only mixing mechanism applicable in laminar microchannel flow, since convective segmentation mechanisms are absent which are characteristic for flows in the turbulent regime. Thus, the generation of alternating laminar sheets by means of geometric constraints (i.e. particular shaping of flows by changes in the microchannel dimensions) is a proper way to achieve good mixing on a microscale. Different concepts have been reported for this purpose, including direct subdivision by splitting (Gravesen, 1997; Richter, 1997) a main stream into a large number of substreams or other indirect means, for example, multiple splitting, drilling or bending which are based on a separation–reunification mechanism (Gravesen, 1996; Hessel, 1995, 1998; Schwesinger, 1996; Wegeng, 1996). Recently, the LIGA-based fabrication of a mixer using direct subdivision has been reported (Richter, 1997). This article gives the first results about the characterization of mixing for this mixer and structurally similar systems.

It was pointed out by different authors that a great potential of such mixers is mixing in extremely short time intervals, that is, in the range of 1 s down to a few milliseconds (Branebjerg, 1996; Wegeng, 1996). This mixing time  $t$  is related to the width of the laminar

sheets  $d_{sh}$  and is proportional to  $d_{sh}^2/D$ ,  $D$  being the diffusion coefficient (Wegeng, 1996). Thus, mixing quality can be strongly improved by the reduction of the sheet width, which is related to structural details of the mixer, mainly the microchannel width  $d_{mc}$ . Today's micromixers fabricated by silicon micromachining and LIGA technologies have channel widths in the range 20–50  $\mu\text{m}$  (Gravesen, 1996; Richter, 1997; Schwesinger, 1996; Wegeng, 1996).

While the performance of some microcomponents such as pumps, heat exchangers, or extractors can be characterized by comparison of standard parameters (e.g. pump frequency, heat transfer coefficient, or volumetric mass-transfer coefficient), a similar procedure for the analysis of mixing is more complicated. The best solution for mixing characterization would be a locally high-resolved in-line measurement of the concentration profiles along the flow axis. Sensors of such small size and fast response time are not available at present. Therefore, the quality of today's micromixers has to be characterized by indirect means. Most often ultrafast acid–base reactions were applied, indicating the extent of mixing by a change of color due to a pH shift (Branebjerg, 1996; Schwesinger, 1996). Since the concentrations of acids and bases vary in each publication and sometimes are not mentioned in detail, the degree of mixing associated with the color change is different for each system. Thus, the comparability of the results as well as their use as an objective measure is very limited. These experiments led to important information about the feasibility of the systems but hardly resulted in any quantitative data due to an insufficient sensitivity and low local resolution.

The aim of our work was to develop and employ a test reaction with high sensitivity and a fast response which is especially adapted for the characterization of micromixers with mixing ratios near 1:1. The method should allow us to employ a correlation between mixing quality and structural details for different mixers. The channel and slit width were varied to shorten diffusion distances and to optimize the flow pattern inside the micromixer. Furthermore, comparisons to macroscopic reference systems were carried out. In addition, this study includes investigations of the parallelization of mixing units to an array. The size of the feeding and collecting

\* To whom correspondence should be addressed. Telephone: 0049-6131-990450. Fax: 0049-6131-990475. E-mail: hessel@imm-mainz.de.

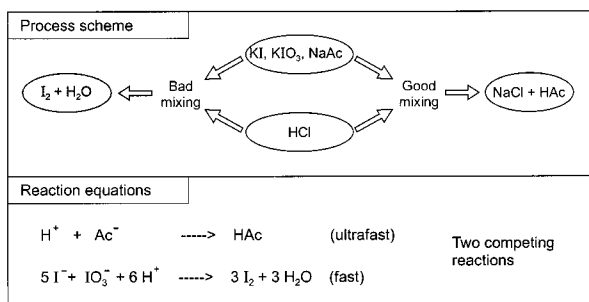


**Figure 1.** Reaction for characterization of mixing quality and feed distribution in continuous-flow micromixers: process scheme and reaction equations. In the case of bad mixing, iodine formation occurs due to a concurrent reaction.

channels of the micromixer array has been optimized in order to achieve homogeneous feed distribution and high mixing efficiency.

Static mini- and micromixers were already successfully used as reaction systems for the performance of very fast chemical reactions in industrial investigations (Krummrad, 1998). Other application fields include the generation of emulsions for pharmaceutical uses, for example, drug delivery, and cosmetics (Löwe, 1998). Furthermore, gas/liquid dispersions generated by static micromixers show large specific interfaces which can be used for processing of diffusive-limited reactions (Hessel 1998). Finally, further potential applications are certainly given for fast mixing, which is an essential operation for gradient HPLC methods as well as for continuous titration or quench-flow analysis (Bökenkamp, 1998).

## Experimental Section

**Characterization of Mixing: Modification of Test Reaction.** We have chosen a method which was originally developed by Villiermaux et al. for the characterization of mixing in continuously stirred batch reactors (Villiermaux, 1991). The batch reactor contained a solution of  $I^-$ ,  $IO_3^-$ , and NaAc (sodium acetate) to which a strong acid was slowly added. The mixing of these two fluids leads to two concurrent reactions (see Figure 1).

The first process is the neutralization of the acid, which is an ultrafast process and will always mask the slower second process, namely the iodine formation, as long as no local excess of the strong acid remains. Such an excess significantly enhances the velocity of the otherwise slow formation of iodine. Thus, local deviations of the average concentration due to an imperfect mixing are detected by iodine formation and can be used to characterize the mixing process. The iodine concentration is measured by UV-vis absorption using a 1 cm cuvette. The higher the absorption due to iodine formation, the worse is the quality of mixing.

In contrast to the batch system of Villiermaux et al., a volume ratio of 1:1 of both fluids is usually applied in the static micromixers described here. Therefore, the concentrations of the solutions had to be modified. In a first experiment the mole numbers of the strong acid (in our case HCl was chosen) and NaAc were maintained as well as the  $I^-$  and  $IO_3^-$  concentrations. This modification resulted in a diluted HCl solution (0.5 wt % or 0.1374 mol/L). However, mixing of these solutions did not result in detectable iodine formation, so that the concentrations of  $I^-$  and  $IO_3^-$  were further increased in

a test series until an acceptable sensitivity was obtained (concentration increase by a factor of 100). The  $H^+$  and NaAc concentrations were maintained. Accordingly, the following three stock solutions resulted: 1 L of a 0.1374 mol/L HCl solution, 0.5 L of a 0.0319 mol/L KI/1.33 mol/L NaAc solution, and 0.5 L of a 0.00635 mol/L  $KIO_3$ /1.33 mol/L NaAc solution. The last two solutions were combined immediately before the start of measurement. The resulting NaAc/KI/ $KIO_3$  and HCl solutions were fed into the micromixer by piston pumps through tubes. UV-vis characterization was performed off-line in a spectrophotometer. The UV-vis spectrum of iodine has two pronounced peaks, of which the peak at 352 nm was chosen for measurement. To minimize the time delay between mixing and measurement, the scan area was limited to 380–330 nm at a speed of 120 nm/min.

Two distinct differences from the experiments of Villiermaux et al. have to be mentioned: First, the iodine formation in an array system is influenced not only by the mixing quality but also by the homogeneity of flow distribution, since a stationary concentration difference due to different volume flows of the individual streams leads to increased iodine formation as well. Thus, in an array system the measurements always represent an overall result of both effects.

Another particular aspect of our modification of the test reaction is a serious limit of its application in the case of long time delays between mixing and measurement. In this case, the amount of iodine formed cannot be exclusively related to the mixing performance (and flow distribution). Since the  $I^-$  and  $IO_3^-$  concentrations have been increased by a factor of 100, the slow, HAc-catalyzed reaction can also result in detectable amounts of iodine even after mixing is completed. The latter effect has been experimentally verified by measuring the time dependence of the absorption of an ideally mixed sample. A linear increase of iodine absorption from 0.04 to 0.5 was observed within about 900 s (15 min). Thus, all measurements were made as fast as possible in order to ensure that the solution did not change significantly.

**Types of Micromixers and Mixing Principle (Multilamination).** Single mixing units are an assembly of three components, namely a LIGA device containing the mixing element which is embedded in a two-piece housing. The LIGA devices are made of nickel on copper (i.e. a nickel layer with microchannels on a copper base plate) or of silver. The stainless steel housing is built of two pieces, the top and bottom plate connected to inlets and outlets (see Figure 2).

The design of the mixing element is based on a layer containing 18 or 15 sinusoidally shaped fluid channels for each fluid with a width of 25 or 40  $\mu\text{m}$ , respectively, and a depth of 300  $\mu\text{m}$  supported by a base plate (see Figure 3). The mixing elements of the mixer array and the single mixing unit are identical.

Here, both fluids enter the single mixing unit via inlet tubes through drilled holes and are thereby fed to distribution voids leading to the microchannels in the LIGA device. The divided substreams in the microchannels penetrate each other but do not contact due to separating walls. To achieve a deep penetration of both fluids (well-defined multilamination) for microchannels of variable depth and width, the pressure loss in this part of the mixer has to be individually adapted. This is performed by restricting the contact area (mixing zone) by a slit on top of the mixing element having variable widths. The slit is connected to the outlet by a

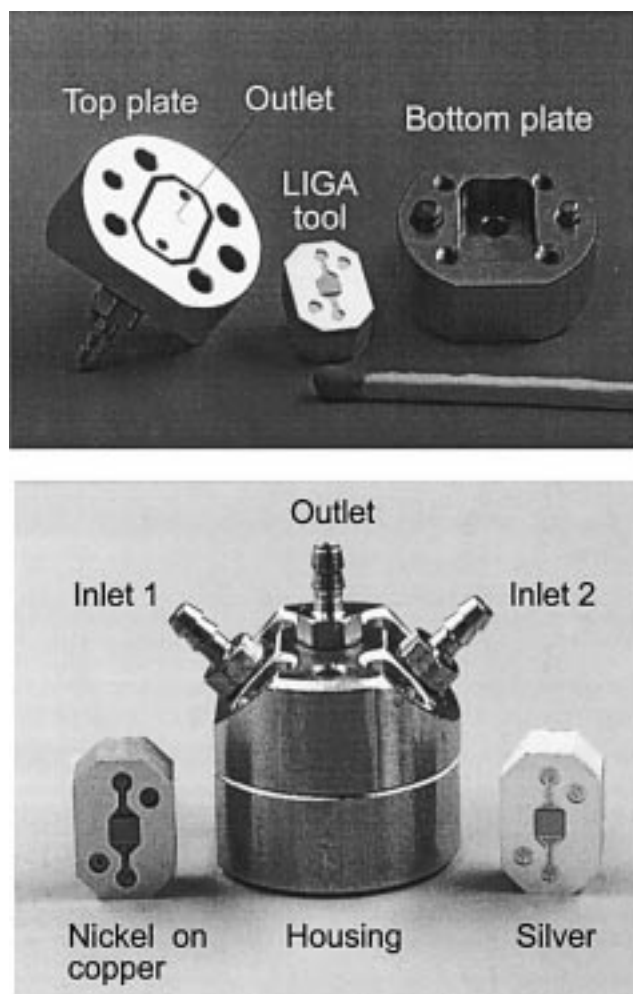


**Figure 2.** Photographs of the single mixing unit: single pieces, LIGA device and housing consisting of top and bottom plates (top image); assembled pieces, housing with inlets and outlets and LIGA devices in nickel on copper and silver (bottom image).

drilled hole of 500  $\mu\text{m}$  diameter which does not break through to the surface facing the microchannels (see Figure 4).

The parallel arrangement of sheets (multilamination) could be proven experimentally: it was found by coincidence that the HCl and ( $\text{I}^-$ ,  $\text{IO}_3^-$ , NaAc) solutions slightly modify the surface of the mixing element made of nickel on copper, probably by oxidation and reduction processes. The difference in reflectivity can be detected by light microscopy investigations. The image in Figure 5 clearly shows a white–black pattern of similar length as compared to the slit width. The edges of the pattern are clearly defined, suggesting a negligible flow in regions beyond the mixing zone. Furthermore, the overlap stretches over the whole mixing zone, thus proving that the flow at the bottom of the microchannels passes the whole mixing zone.

In the mixer array, one fluid enters the mixer array via one inlet tube through a drilled hole to a circular ring (see Figure 6).

On this ring, 10 feed lines branch to 10 equal mixing elements. The other fluid is guided through a drilled hole to the center of the LIGA device, from which it is distributed to the mixing elements. The mixing zone is given by a dodecagon-shaped channel of variable width (350 or 2000  $\mu\text{m}$ ) in the top plate. A drilled hole of 500  $\mu\text{m}$  diameter connects this channel to the outlet. Op-

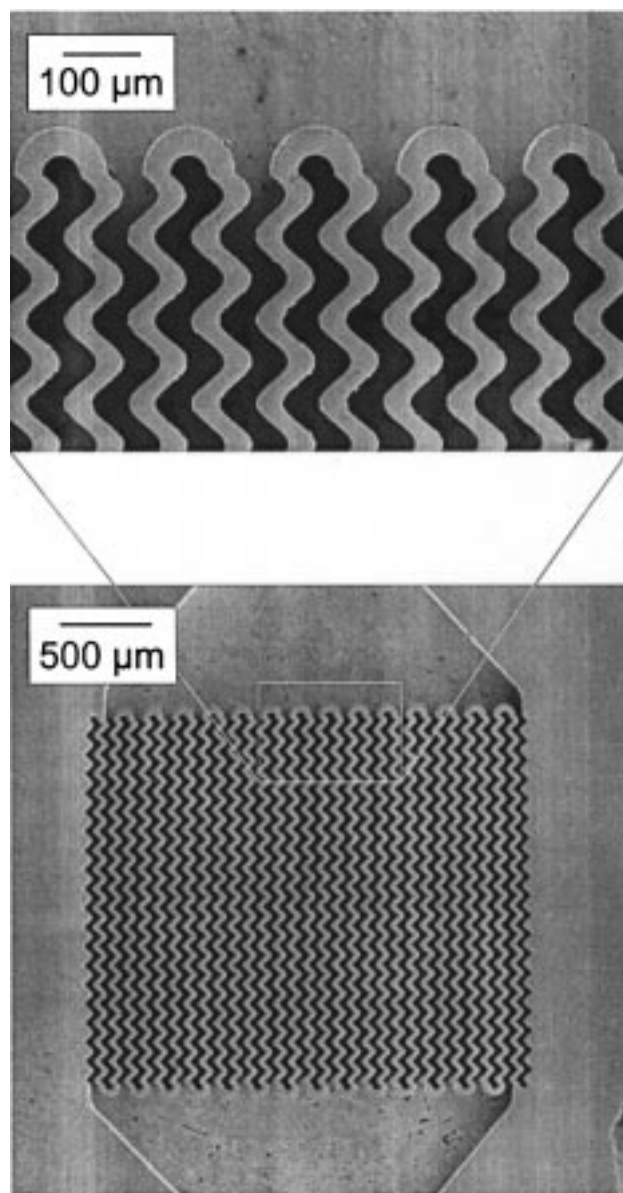


**Figure 3.** SEM images of one mixing element within the mixer array (2  $\times$  15 single channels) and magnification showing nine single channels. The width of the channels varies over a certain range due to their sinuoidal shape, so that 40  $\mu\text{m}$  represents only an average value. The same is true for the mixing element with channels of 25  $\mu\text{m}$  width.

tionally, the volume of the outlet ring can be significantly increased by micromilling of an additional channel in the top plate (increase of channel height). This should result in an equilibration of the individual pressure losses of the feeding lines.

The pressure loss curves of the single mixing unit and mixer array are shown in Figure 7.

A volume flow of 1 L/h for each fluid is achievable in the single mixing unit using aqueous solutions at a pressure loss of 1700 hPa, while for the mixer array a limit of 3 L/h is found at about 1200 hPa. Thus, the flow normalized to one mixing element is about 4 times higher for the single mixing unit than for the mixer array at similar pressure loss. This demonstrates that the pressure loss is influenced not solely by the microstructured parts (which are identical) but also by the precision-engineered parts of the housing with varying inlet and outlet rings and holes. Furthermore, turbulent flow sections in the inlet and outlet elements of the



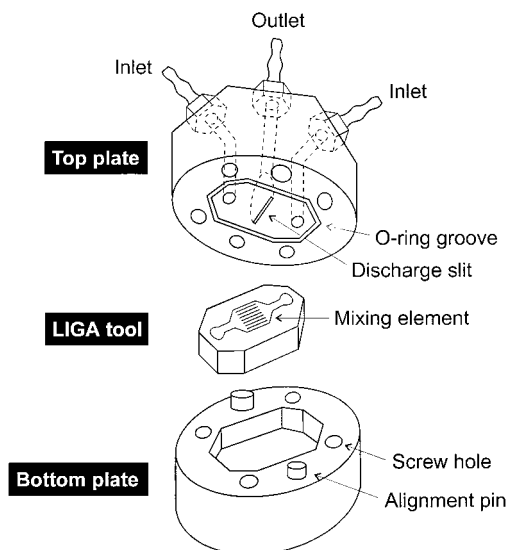


Figure 4. Explosion drawing of the single mixing unit.

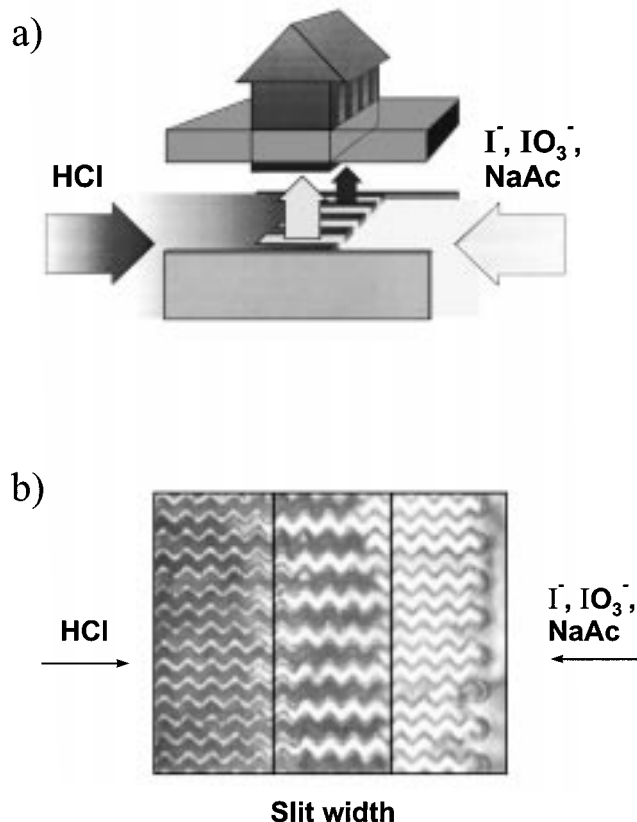


Figure 5. (a) Schematic representation of the multilamination principle using the LIGA micromixer. (b) Light microscopic image of the mixing zone after exposure of the mixing elements to HCl and ( $\text{I}^-$ ,  $\text{IO}_3^-$ , NaAc) reactant solutions.

housing cause a nonlinearity of both pressure loss curves. For a pure laminar system a linear relationship should be expected.

**Fabrication of the Single Mixing Unit and Micromixer Array: Fabrication of the LIGA Devices.** The LIGA devices of the single mixing unit and the micromixer array were fabricated by the first two steps of the LIGA process, namely deep X-ray lithography and electroforming (Ehrfeld, 1994; Löwe, 1994; Weber 1996). The channels were sinusoidally shaped, resulting in a high mechanical stability of the resist walls during the fabrication process, thus enabling the production of

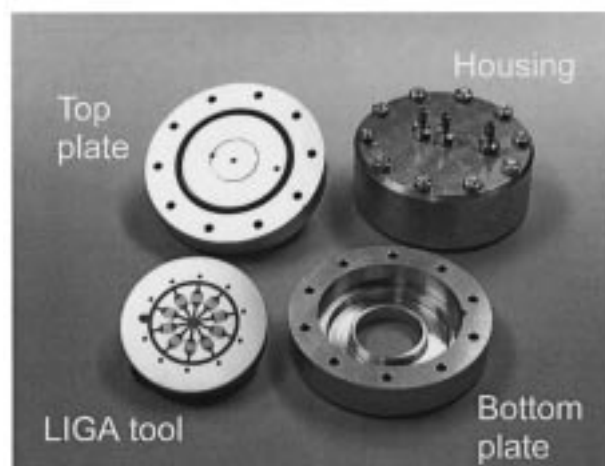
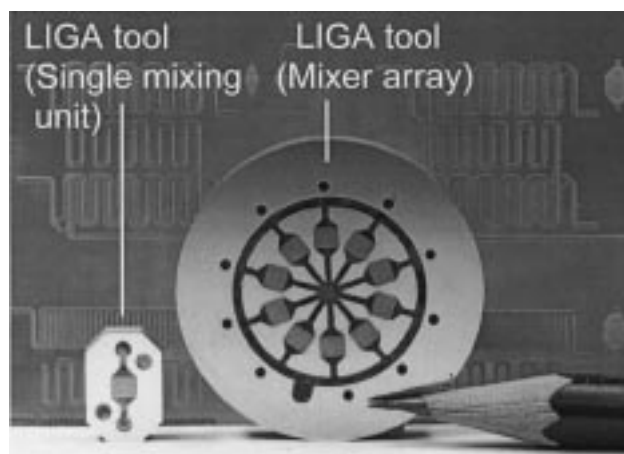


Figure 6. Photographs of the mixer array: mixing parts made by an electroforming process in the frame of the LIGA process, single mixing unit and mixer array (top image); single and assembled pieces of the mixer array, mixer and housing consisting of top and bottom plates (bottom image).

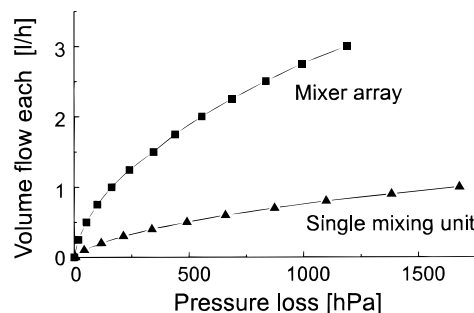
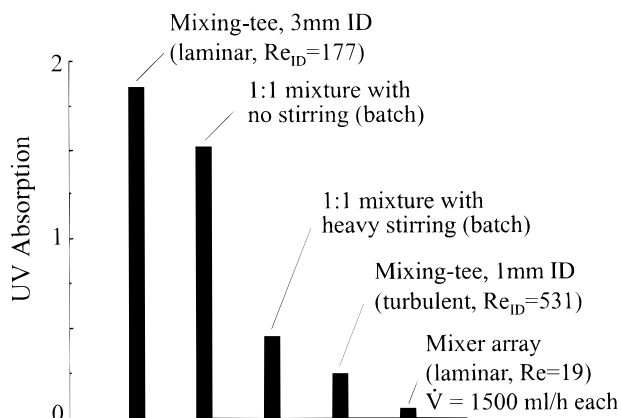


Figure 7. Pressure loss curve for the single mixing unit and a mixer array having a channel width of  $40\ \mu\text{m}$  and a depth of  $300\ \mu\text{m}$ . For the mixer array the pressure loss was measured between the interior inlet and the outlet.

mixer structures with high aspect ratios. Two types of LIGA devices were realized, the first having a channel width of  $25\ \mu\text{m}$  and the second with  $40\ \mu\text{m}$ .

**Fabrication of the Housing.** The housing of the micromixers was fabricated of stainless steel by conventional precision engineering applying drilling, micromilling, or  $\mu$ -EDM techniques. For the mixer array the outlet ring (mixing zone) was fabricated by micromilling, while for the single mixing unit microelectro discharge machining ( $\mu$ -EDM) using a rotating electrode was applied ( $60\ \mu\text{m}$  width of mixing zone). Mechanical sealing was performed between the top plate and the



**Figure 8.** Absorption versus wavelength: Comparison of mixing of mixer array having a channel width of  $40\ \mu\text{m}$  and a depth of  $300\ \mu\text{m}$  to that of batch and continuous-flow macrosystems at a fixed volume flow of  $1500\ \text{mL/h}$  for each inlet.

mixer array (LIGA device) by tight contact of polished surfaces and, against the environment, by an O-ring surrounding the mixing element. The housing was designed to withstand pressures up to 30 bar and was equipped with connectors for the fluids.

## Results

**Mixing Characteristic of the Mixing Element and Comparison to Other Systems.** The characterization of mixers by the method described here is only relative and cannot be directly related to a mixing time. Therefore, reference systems of known good or bad mixing quality have been chosen for comparison. In Figure 8 the mixing quality of micromixers having a channel width of  $40\ \mu\text{m}$  is compared to those of batch as well as continuous-flow macrosystems.

As batch systems, glass vessels (beakers) were taken, being stirred by standard laboratory impellers. Similar to the experimental setup of Villiermaux et al., the HCl solution was added dropwise to a beaker containing the whole volume of the  $\text{I}^-/\text{IO}_3^-/\text{NaAc}$  solution. As expected, mixing is strongly improved by the aid of stirring for the batch system. The mixer array provides a much better mixing quality. The macroscopic mixing-tees used were continuous-flow systems with similar dimensions of inlets and outlets to those of the micromixers. Thus, by small variations of the inner diameter (at constant volume flow), measurements in both the turbulent and laminar regimes were possible. Mixing in the mixing-tees was much better in the turbulent compared to the laminar regime (as expected). The mixer array, although in the laminar regime, still had a much better performance than the mixing-tees, in either the laminar or turbulent regime.

**Multilamination and Flow Distribution in Mixer Arrays.** The design of the micromixer enables a simple strategy for optimization of mixing performance for any value of flow velocity or volume flow by simple exchange of two pieces: the upper part of the housing defining the slit width and the LIGA device defining the microchannel height and width. The enormous impact of these parameters is shown in Figure 9.

A micromixer with a large slit width of  $2000\ \mu\text{m}$  and microchannels of  $40\ \mu\text{m}$  width and  $300\ \mu\text{m}$  depth shows a nonoptimal mixing performance. Limiting the opening area by a narrow slit of  $350\ \mu\text{m}$  width results in optimal mixing. Once the optimal solution has been found for a

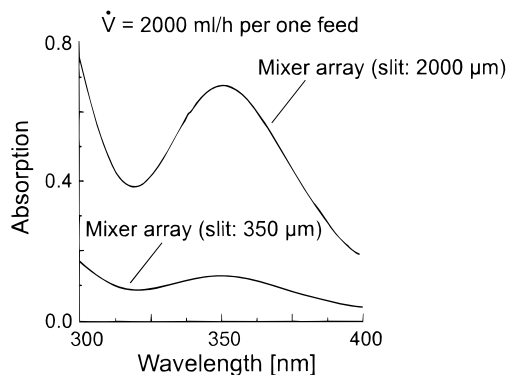


**Figure 9.** Absorption versus wavelength: Comparison of mixing of a standard mixer array (slit width:  $350\ \mu\text{m}$ ) to that of a mixer array with a slit width of  $2000\ \mu\text{m}$  at a fixed volume flow of  $2000\ \text{mL/h}$  for each inlet, both having a channel width of  $40\ \mu\text{m}$  and a depth of  $300\ \mu\text{m}$ .

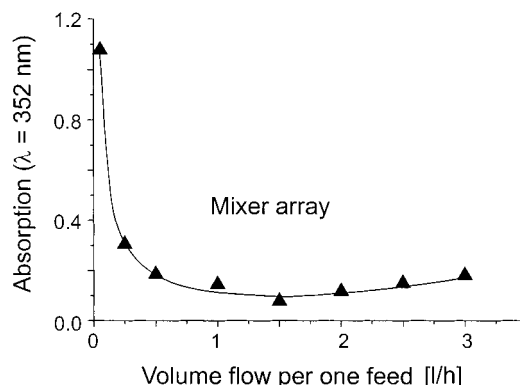


**Figure 10.** Absorption at  $352\ \text{nm}$  versus volume flow for a mixer array having a channel width of  $40\ \mu\text{m}$  and a depth of  $300\ \mu\text{m}$ . The values for the volume flow are related to each of the entering fluids.

single unit, a further increase in volume flow can be achieved by parallelization of single units. Indeed, Figure 10 reveals that low values of iodine concentration and, consequently, a good mixing performance are obtained for the mixer array over a wide range of volume flow.

A minimum of absorption can be detected at  $1500\ \text{mL/h}$  as well as a weak increase to the maximum flow of  $3000\ \text{mL/h}$ . A more pronounced increase in absorption can be observed for smaller values of volume flow, especially in the region  $50\text{--}100\ \text{mL/h}$ .

The mixing quality in mixer arrays can be further optimized by careful control of the homogeneity of the flow distribution toward the individual units. In the present design this was performed by an increase of the cross section of the inlet ring. Thereby, pressure differences of feed lines resulting from different distances to the inlet hole were equilibrated. Figure 11 shows that the mixer array with the larger cross section of the inlet ring exhibits a better mixing performance, in particular in the region  $500\text{--}2000\ \text{mL/h}$ .

In Figure 12 the mixing quality of a thus optimized mixer array is compared to that of an optimized single mixing unit, both having a channel width of  $40\ \mu\text{m}$ . For a better comparison the overall volume flow has been normalized to a single mixing element.

The mixing qualities are similar for normalized volume flows up to  $200\ \text{mL/h}$ . Actually, the mixer array seems to be better here, but this is probably caused by the different contribution of undesired iodine formation

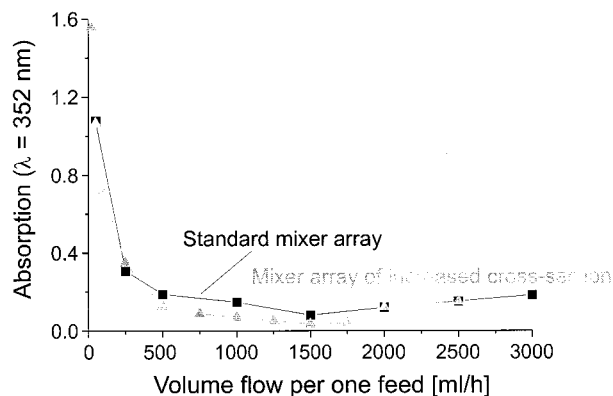


**Figure 11.** Absorption at 352 nm versus volume flow: Comparison of mixing of a standard mixer array to that of a mixer array having a channel width of 40  $\mu\text{m}$  and a depth of 300  $\mu\text{m}$  with an inlet ring of increased cross section.

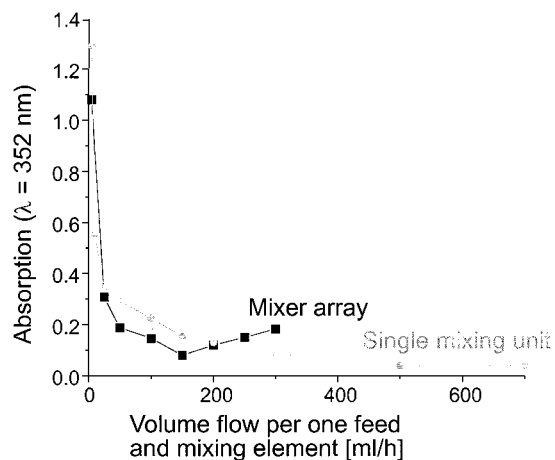


**Figure 12.** Absorption at 352 nm versus volume flow: Comparison of mixing of a mixer array to that of a single mixing unit having a channel width of 40  $\mu\text{m}$  and a depth of 300  $\mu\text{m}$ . The volume flow of the mixing array was normalized to a single element to allow a better comparison to the single mixing unit.

after mixing due to different time intervals between mixing and the start of the UV-vis measurement. For flows higher than 200 mL/h the single mixing unit shows a better mixing performance than that of the mixer array. Nevertheless, even the best value at 700 mL/h is only slightly different from the best value of the mixer array at 200 mL/h. Since this corresponds to an overall flow of 2 L/h, this proves that parallelization of flows can be combined with optimized mixing.

The absence of the increase in absorption at high volume flows for single units shows that a small contribution of flow inhomogeneities is present in mixer arrays. In the Discussion it will be outlined in detail that back mixing effects due to turbulences in the collecting ring equilibrate this effect at low volume flows. The monotonic increase of absorption at low volume flow for both single units and arrays is due to the increased time interval until the start of the UV-vis measurement.

**Variation of Microchannel Width.** In the last sections it was described how the optimization of mixing quality for single mixing units can be achieved by proper combination of slit and microchannel width. The latter was always fixed to 40  $\mu\text{m}$ . In this chapter the influence of the reduction of microchannel width is analyzed. Figure 13 shows the characterization of the single

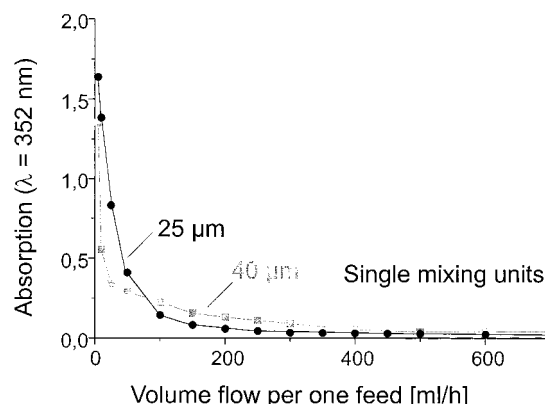


**Figure 13.** Absorption at 352 nm versus volume flow: Comparison of mixing of single mixing units with that of mixing elements of 25 and 40  $\mu\text{m}$  and a depth of 300  $\mu\text{m}$ .

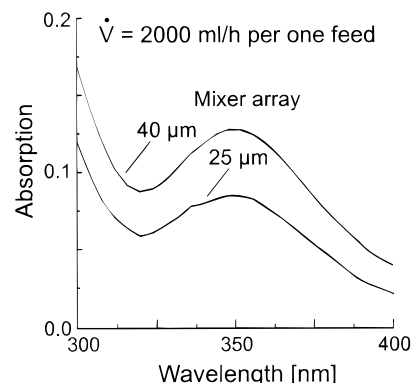


**Figure 14.** Absorption versus wavelength: Comparison of mixing of mixer arrays with mixing elements of 25 and 40  $\mu\text{m}$  channel widths and a depth of 300  $\mu\text{m}$  at a fixed volume flow of 2000 mL/h for each inlet.

mixing unit having microchannel widths of 40 and 25  $\mu\text{m}$  (the slit width was in both cases 60  $\mu\text{m}$ ).

Indeed, the mixing performance of the 25  $\mu\text{m}$  mixer is significantly improved over the whole flow range compared to that of the 40  $\mu\text{m}$  mixers.

Similar findings have been made for the mixer array. In Figure 14 the absorption values for the 25 and 40  $\mu\text{m}$  mixer arrays at a fixed volume flow of 2000 mL/h are shown.

It cannot be checked by the experimental method used here if the measured data are in accordance with the  $d^2$ -dependence of  $t$ . However, possible deviations may be caused by differences of the actual layer thickness from the channel width, for example, by the non-negligible thickness of the separating walls. Furthermore, the number of available slit widths was limited so that combinations of the microchannel and slit width different from 40/60 and 25/60 may yield a still better performance.

## Discussion

**Mixing Quality and Pressure Loss.** An ideal micromixer based on multilamination would combine excellent mixing quality and high throughput. This implies the formation of homogeneous fluid sheets having ultrathin thickness as well as large length and height. However, an inherent characteristic of the mixing principle described here is that both parameters are not independent but are inversely related to each other. This is caused by the necessity to guide the fluid



through the mixing element in order to achieve a uniform outflow of the microchannels. If the mixing zone is significantly larger than the microchannel width, a nonuniform flow will occur, resulting only in a partial overlap of the sheets. The consequence is a nonideal mixing process, as measured in Figure 9.

The experimental results show that by proper combination of slit and microchannel width a good mixing performance can be achieved over a large range of volume flow, even if only a single mixing unit is used. The light microscopy image of Figure 5 shows a sharply edged pattern of alternating sheets and thus demonstrates a full overlap. The consequence is a high mixing quality, as evidenced by the comparison to macroscopic systems (stirred batch vessels and mixing tees). It has to be pointed out that the mixing quality of this laminar-flow microsystem is much better than that in the reference systems having a turbulent regime (see Figure 8).

**Mixing Quality and Parallelization of Mixing Elements.** For many applications of microreactors, a high volume flow of the reactants is desired. To a certain extent, this can be realized by increasing the channel depth in one single mixing unit of the present design. However, this solution has technical limits. For very high volume flows the increase of the number of microchannels by parallelization of mixing units is the adequate solution. For the mixer arrays described here, good mixing quality is not limited to a narrow range of volume flow, but, on the contrary, a nearly constant quality over a large range of volume flow is found (500–3000 mL/h; see Figures 10 and 11). Thus, parallelization of mixing enables increased volume flow in a region ( $> 700$  mL/h) which cannot be realized using one single mixing unit. On the other hand, a single mixing unit enables efficient mixing in the low volume flow regime (2–500 mL/h; see Figure 12).

**Mixing Quality and Volume Flow.** A fully laminar system should give a constant mixing quality over the whole flow range (level a in Figure 15). Instead, for the mixer array a rather complex dependency of the iodine formation on the volume flow was found. An explanation for this behavior has to consider stepwise the effect of certain deviations of the experiment from the theoretically expected behavior (curves a–e in Figure 15).

Inhomogeneities in the flow distribution result for both types of mixers in an increased iodine absorption (level b). This effect is much more pronounced for the mixer array, thereby yielding a higher value for level b. Different values of level b can even be detected for mixer arrays of different design: the array with the inlet ring volume of increased cross section showed lower absorption values compared to those of the standard mixer array in the region of medium volume flow (see Figure 11).

The experimental data measured at high volume flows correspond to the constant value given by level b (at least for the single mixing unit; see discussion below). At low volume flows the values of absorption increase, since slow iodine formation occurs due to longer time delays between mixing and measurement (curve c). This effect has been experimentally verified by measuring the time dependence of the absorption of an ideally mixed sample: a sample was mixed in the single mixing unit at high volume flow (600 mL/h), and the absorption  $A$  was monitored versus the time  $t$ . A linear relationship resulted ( $A \sim t$ ), so that curve c

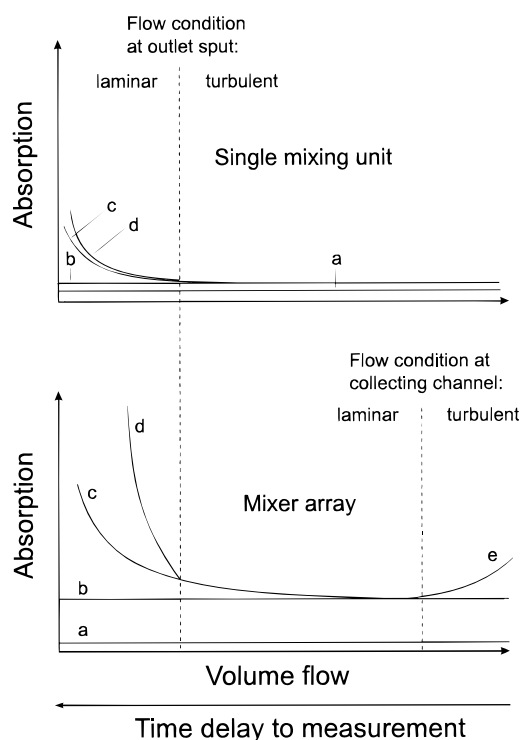


**Figure 15.** Theoretical behavior of the mixer array: (a) mixing without subsequent equilibration and with homogeneous flow distribution; (b) mixing without subsequent equilibration and with inhomogeneous flow distribution; (c) mixing with subsequent equilibration and with inhomogeneous flow distribution with a parasitic mixing effect; (d) mixing with subsequent equilibration and with inhomogeneous flow distribution with partial absence of the parasitic mixing effect; (e) mixing with turbulent flow in the outlet spout.

should give a  $1/t$  dependence of the absorption (volume flow  $\sim 1/t$ ). Experimental data measured at high volume flow fit this theory (experimental curve  $\sim$  theoretical curve c), but at low volume flow a considerable deviation is abruptly observed (experimental curve  $\sim$  curve d). This behavior may be caused by a change from turbulent to laminar flow at the outlet connector, the so-called parasitic mixing, which is indicated from calculations of the corresponding Reynolds numbers. This additional mixing process can assist the overall mixing performance if deviations from flow homogeneity are present. The parasitic effect is missing at low volume flow and, hence, leads to a further increase of iodine absorption from curve c to curve d. The experimental data prove that the deviations of curves c and d are much stronger for the mixer array because of the higher flow inhomogeneity (given by curve b).

At high volume flows deviations of the experimental data from curve d are only found for the mixer arrays (curve e). This phenomenon is at present not well understood but may be related to pressure fluctuations caused by turbulences in the collecting channel creating an undefined flow pattern within the mixing elements and, thereby, enhancing the iodine formation.

**Mixing Time.** The mixing time cannot be directly measured by the test reaction. Instead a comparison was made for mixing elements having various channel widths (see Figures 13 and 14). It is evident that a decrease of channel width shortens the mixing time. The use of the LIGA technique allows a further decrease of the channel width much below  $25\ \mu\text{m}$ , so that for special applications the mixing quality can still be improved.

Even for such small channel sizes, high volume flows can be achieved by increasing the number of channels in one mixing element.

### Acknowledgment

The authors would like to thank A. Wolf for performing the  $\mu$ -EDM techniques, K. Gebauer for preparing the LIGA devices by electroforming, D. Erntner and C. Hofmann for the construction of the housings, and A. Woisnitza and S. Dück for the UV-vis characterization of mixing.

### Literature Cited

- Benson, R. S.; Ponton, J. W. Process miniaturization—a route to total environmental acceptability? *Trans. Inst. Chem. Eng.* **1993**, *A71*, 160.
- Bökenkamp, D.; Desai, A.; Yang, X.; Tai, Y.-C.; Marzluff, E. M.; Mayo, S. L. Micro fabricated silicon mixers for submillisecond quench-flow analysis. *Anal. Chem.* **1998**, *70*, 232.
- Branebjerg, J.; Larsen, U. D.; Blankenstein, G. Fast mixing by parallel multilayer lamination. In *Proceedings of the 2nd International Symposium on Miniaturized Total Analysis Systems  $\mu$ TAS96*, Basel; Widmer, H. M., Verpoorte, E., Barnard, S., Eds.; special issue of *Anal. Meth. Instrum.*; 1996; pp 228–230.
- Ehrfeld, W.; Lehr, H. Synchrotron Radiation and the LIGA-Technology. *Synchrotron Radiat. News* **1994**, *7*, 9.
- Ehrfeld, W.; Hessel, V.; Löwe, H.; Richter, Th. Anwendungspotentiale für chemische und biologische Mikroreaktoren *Chem.-Ing. Tech.* **1996**, *68* (9), 1091.
- Ehrfeld, W.; Hessel, V.; Möbius, H.; Richter, Th.; Russow, K. Potentials and Realization of Micro Reactors. In *Microsystem Technology for Chemical and Biological Microreactors; DECHEMA monograph*; Verlag Chemie: Weinheim, 1996; Vol. 132.
- Gravesen, P.; Branebjerg, J.; Krog, J. P.; Nielsen, C. R. Fast mixing by lamination. *Proceedings of IEEE MEMS'96*, San Diego, CA; 1996.
- Hessel, V.; Ehrfeld, W.; Möbius, H.; Richter, Th.; Russow, K. Potentials and realization of microreactors. *Proceedings of the International Symposium on Microsystems, Intelligent Materials and Robots*, Sendai, Japan; 1995; p 45.
- Hessel, V.; Ehrfeld, W.; Golbig, K.; Haverkamp, V.; Löwe, H.; Richter, Th. Gas/liquid dispersion processes in micromixers: the hexagon flow. In *Proceedings of the 2nd International Conference on Microreaction Technology*, Topical Conference Preprints, March 9th–12th, 1998, New Orleans; Ehrfeld, W., Rinard, I. H., Wegeng, R. S., Eds.; 1998; pp 259–266.
- Hönicke, D.; Wiessmeier, G. Heterogeneously catalyzed reactions in a microreactor. In *Microsystem Technology for Chemical and Biological Microreactors DECHEMA monograph*; Verlag Chemie: Weinheim, 1996; Vol. 132, p 93.
- Kämper, K.-P.; Ehrfeld, W.; Döppler, J.; Hessel, V.; Lehr, H.; Löwe, H.; Richter, Th.; Wolf, A. Microfluidic components for biological and chemical microreactors. *Proceedings of the IEEE MEMS'97*, Nagoya, Japan, 1997.
- Krummradt, H.; Koop, U.; Stoldt, J. Mikro- und Minireaktoren für verfahrenstechnische Prozesse. *Chem.-Ing. Tech.* **1998**, *70* (9), 1074.
- Lerou, J. J.; Harold, M. P.; Ryley, J.; Ashmead, J.; O'Brien, T. C.; Johnson, M.; Perrotto, J.; Blaisdell, C. T.; Rensi, T. A.; Nyquist, J. Microfabricated minichemical systems: Technical feasibility. In *Microsystem technology for chemical and biological microreactors, DECHEMA Monographs*; Verlag Chemie: Weinheim, 1996; Vol. 132, p 51.
- Löwe, H.; Mensinger, H.; Ehrfeld, W. Galvanoformung in der LIGA-Technik. *Jahrbuch Oberflächentechnik*; Metall Verlag: Heidelberg, 1994; Vol. 50, p 11.
- Löwe, H.; Hessel, V.; Ehrfeld, W.; Golbig, K.; Haverkamp, V.; Richter, Th. Mehrphasenprozesse in Mikroreaktoren—Konzept, Systeme, Charakterisierung. *Chem.-Ing. Tech.* **1998**, *70* (9), 1074.
- Mathies, R. A.; Woolley, A. T. Ultrahigh-speed DNA sequencing using capillary electrophoresis chips. *Anal. Chem.* **1995**, *67* (20), 3676.
- Mensinger, H.; Richter, Th.; Hessel, V.; Döppler, J.; Ehrfeld, W. Microreactor with integrated static mixer and analysis system. In *Micro Total Analysis Systems*; van den Berg, A., Bergveld, P., Eds.; Kluwer Academic Publishers: Dordrecht, 1995; p 237.
- Möbius, H.; Ehrfeld, W.; Hessel, V.; Richter, Th. Sensor controlled processes in chemical microreactors. In *Transducers '95—Eurosensors IX, Proceedings of the 8th International Conference on Solid-State Sensors and Actuators/Eurosensors IX*, Stockholm, 1995; p 775.
- Richter, Th.; Löwe, H.; Ehrfeld, W.; Golbig, K.; Hessel, V. Anwendungspotentiale für chemische und biologische Mikroreaktoren, *Chem.-Ing. Tech.* **1997**, *69* (7), 931.
- Schubert, K.; Bier, W.; Keller, W.; Linder, G.; Seidel, D. Gas-to-gas heat transfer in micro heat exchangers. *Chem. Eng. Process.* **1993**, *32* (1), 33.
- Schwesinger, N.; Frank, T.; Wurmus, H. A modular microfluid system with an integrated micromixer. *J. Micromech. Microeng.* **1996**, *6*, 99.
- Shaw, J.; Miller, B.; Turner, C.; Harper, M.; Graham, S. Mass transfer of species in micro-contactors: CFD modelling and experimental validation. *Proceedings of the 2nd international symposium on miniaturized total analysis systems,  $\mu$ TAS 96*, Basel; Widmer, H. M., Verpoorte, E., Barnard, S., Eds.; 1996; p 185.
- Villiermaux, J.; Falk, L.; Fournier, M.-C.; Detrez, C. Use of parallel competing reactions to characterize micromixing efficiency. *AIChE Symp. Ser.* **1991**, *286* (88), 6.
- Weber, L.; Ehrfeld, W.; Freimuth, H.; Lehr, H.; Pech, B. Micro molding—a powerful tool for the large scale production of precise microstructures. *Proc. SPIE—Int. Soc. Opt. Eng.* **1996**, *2879*, 156.
- Wegeng, R. W.; Call, C. J.; Drost, M. K. Chemical system miniaturization. *Proceedings of 1996 Spring National Meeting AIChE*, New Orleans, 1996; p 1.
- Widmer, H. M.; Verpoorte, E. M. J.; van der Schoot, B. H.; Jeanneret, S.; Manz, A.; de Rooij, N. F. Three-dimensional micro flow manifolds for miniaturized chemical analysis systems. *J. Micromech. Microeng.* **1994**, *4*, 246.

Received for review March 2, 1998

Revised manuscript received November 3, 1998

Accepted November 20, 1998

IE980128D